Cardiovascular Toxicology (2020) 20:548–556
https://doi.org/10.1007/s12012-020-09580-8

Effects of Extracellular Matrix Softening on Vascular Smooth Muscle Cell Dysfunction

Yihui Shao[1,2,3] · Guoqi Li[2,3] · Shan Huang[2,3] · Zhenfeng Li[4] · Bokang Qiao[2,3] · Duanduan Chen[4] · Yulin Li[2,3] · Huirong Liu[1] · Jie Du[2,3] · Ping Li[2,3]

Published online: 4 June 2020

Abstract

Vascular smooth muscle cells (VSMCs) shift from a physiological contractile phenotype to an adverse proliferative or synthetic state, which is a major event leading to aortic disease. VSMCs are exposed to multiple mechanical signals from their microenvironment including vascular extracellular matrix (ECM) stiffness and stretch which regulate VSMC contraction. How ECM stiffness regulates the function and phenotype of VSMCs is not well understood. In this study, we introduce in vitro and in vivo models to evaluate the impact of ECM stiffnesses on VSMC function. Through unbiased transcriptome sequencing analysis, we detected upregulation of synthetic phenotype-related genes including osteopontin, matrix metalloproteinases, and inflammatory cytokines in VSMCs cultured using soft matrix hydrogels in vitro, suggesting VSMC dedifferentiation toward a synthetic phenotype upon ECM softening. For the in vivo model, the lysyl oxidase inhibitor β-aminopropionitrile monofumarate (BAPN) was administrated to disrupt the cross-linking of collagen to induce ECM softening. Consistently, decreased ECM stiffnesses promoted VSMC phenotypic switching to a synthetic phenotype as evidenced by upregulation of synthetic phenotype-related genes in the aortas of mice following BAPN treatment. Finally, BAPN-treated mice showed severe expansion and developed aortic dissection. Our study reveals the pivotal role of ECM softening in regulating the VSMC phenotype switch and provides a potential target for treating VSMC dysfunction and aortic dissection disease.

Keywords Extracellular matrix · Vascular smooth muscle cell · Synthetic phenotype

Introduction

Vascular smooth muscle cells (VSMCs) are key cells in the vascular wall and are responsible for regulating blood vessel homeostasis [1]. VSMCs have diverse function and phenotype depending on their environmental cues [2]. Switching of VSMCs from a physiological contractile phenotype to an adverse proliferative, synthetic and inflammatory state is a major initiating event leading to atherosclerosis or aortic aneurysm disease [3, 4]. Multiple mechanical cues including extracellular matrix stiffness and stretch regulate VSMCs contraction [5]. The ECM of vascular wall functions not only as a scaffold for the anchorage and mobility of VSMCs but also impart mechanical cues to VSMCs to regulate the shape, metabolism, migration, proliferation, and differentiation of VSMCs [6–8]. Thus, the integrity of and signaling in the ECM are essential for VSMC function and blood vessel homeostasis, and aberrations in the ECM can lead to the onset and development of various diseases.

Handling editor: Yu-Ming Kang

✉ Huirong Liu
liuhr2000@ccmu.edu.cn

✉ Jie Du
jiedu@ccmu.edu.cn

✉ Ping Li
doctorliping7511@sohu.com

[1] Department of Physiology and Pathophysiology, School of Basic Medical Sciences, Capital Medical University, Beijing 100069, China

[2] Beijing Anzhen Hospital Affiliated to Capital Medical University, Beijing 100029, China

[3] Beijing Institute of Heart, Lung, and Blood Vessel Diseases, Beijing Anzhen Hospital Affiliated to Capital Medical University, Beijing 100029, China

[4] School of Life Science, Beijing Institute of Technology, Beijing 100081, China

The physical properties of the ECM, including density, rigidity, and insolubility [9–11]are sensed by cells, which leads to various changes in cell function and phenotype [12]. For example, a soft ECM prevents the formation of stable cell–cell adherens and induces the formation of invadosome-like protrusions, leading to cellular invasiveness [13]. In contrast, fibroblasts develop an activated myofibroblast phenotype with α-smooth muscle actin activity in stiffened fibrous tissues [14]. Whether changes in ECM stiffness in the vascular wall regulate the VSMC phenotype remains unclear.

In this study, we used in vitro and in vivo models to evaluate the impact of ECM stiffnesses on the phenotype and function of VSMCs. Matrix stiffness was regulated in vitro by using reconstituted matrix hydrogel containing a mix of Matrigel and collagen I, where their concentrations were changed to obtain stiff or soft ECM. We observed that soft ECM induced a synthetic phenotype of VSMCs. Consistently, in the in vivo model in which β-aminopropionitrile monofumarate (BAPN) was administered to young mice to reduce ECM stiffness in the vascular wall, we observed VSMC dedifferentiation toward a synthetic phenotype, which is a key event in the pathogenesis of vascular remodeling-related disease.

Materials and Methods

Cell Culture

Mouse VSMCs were isolated from the thoracic aortas of 8-week-old C57BL/6 male mice as described previously [15]. Briefly, thoracic aortas were isolated from euthanized mice under sterile conditions followed by digestion in 100 µL of Type I collagenase (Worthington CLS-1, 1 mg/mL) solution at 37 °C for 15 min. Following digestion, the aortas were sliced into ~ 1–2-mm pieces and placed in a 6-well plate, in which they were cultured in Dulbecco's modified Eagle's medium (DMEM), supplemented with 20% fetal bovine serum (FBS), ITS Premix Universal Culture Supplement, human epidermal growth factor (hEGF), and 1% penicillin–streptomycin, at 37 °C in a humidified atmosphere of 95% air/5% CO_2. On commencing proliferation and attachment to the plate surface, the VSMCs were trypsinized and expanded. Cultured cells were identified as VSMCs based on morphology and staining for smooth muscle cell differentiation markers. Cells between passages 3 and 6 were used in all experiments.

Three-Dimensional Cell Culture

Three-dimensional cell culture was performed as previous described [16–18]. Cells were embedded in a mixture of Growth Factor Reduced Matrigel (BD Biosciences, USA) and Collagen I (Trevigen, USA). The Collagen I solution was then mixed on ice with Matrigel to obtain a final concentration of 3 mg/mL (stiff matrix) or 1.2 mg/mL (soft matrix). VSMCs were trypsinized, counted, and then resuspended in growth medium. Thereafter, the cells were mixed with Matrix hydrogel in a 1:1 (v/v) ratio. Twelve-well plates were pre-coated with 0.5 mL of cell-free 50% medium/50% Matrix hydrogel, followed by gelling at 37 °C in a cell incubator. After gelling, cells were seeded on the Matrix hydrogel and cultured in normal growth medium, which was changed at 2-day interval during the experiments.

RNA Sequencing

For sequencing purposes, we used 3-µg aliquots of RNA for sample preparation. Sequencing libraries were generated and sequenced using an Illumina Hiseq platform (Novogene, China) and 125-bp/150-bp paired-end reads were generated. Feature Counts v1.5.0-p3 was used to count the number of reads mapped to each gene. Differential expression analysis of two conditions/groups was performed using the DESeq2 R package (1.16.1). Genes with an adjusted P value < 0.05 were assigned as differentially expressed (DEGs). Gene ontology (GO) enrichment analysis of the DEGs was implemented using the cluster Profiler R package, in which gene length bias was corrected. GO terms with a corrected P value < 0.05 were considered significantly enriched with DEGs. Pathway analysis, predominantly based on the Kyoto Encyclopedia of Genes and Genomes (KEGG) database, was employed to determine the statistical enrichment of DEGs in KEGG pathways.

Quantitative Real-Time PCR

Total RNA was isolated from cultured cells or mice aortic samples using TRIzol (Invitrogen) according to the manufacturer's instructions. The isolated RNA was converted to cDNA using a GoScript reverse transcription kit (Promega, USA). qRT-PCR was performed using a SYBR Green Master Mix (Takara, Japan) and an iCycler iQ system (Bio-Rad, USA). The level of target gene expression was normalized against the *GAPDH* gene. The primer sequences used for amplification are listed in Table 1.

Western Blotting

VSMCs were collected and lysed using lysis buffer (T-PER; Thermo Fisher Scientific, Waltham, USA) containing a protease inhibitor cocktail and phosphatase inhibitors (Roche Applied Science, Germany). Protein samples (20–40 µg per lane) were subjected to SDS-PAGE and transferred to nitrocellulose membranes. The membranes were subsequently

Table 1 A list of PCR primers used in this study

Genes	Forward primer 5′ to 3′	Reverse primer 5′ to 3′
OPN	AGCAAGAAACTCTTCCAAGCAA	GTGAGATTCGTCAGATTCATCCG
KLF5	CCGGAGACGATCTGAAACACG	GTTGATGCTGTAAGGTATGCCT
vimentin	CGTCCACACGCACCTACAG	GGGGGATGAGGAATAGAGGCT
MMP3	ACATGGAGACTTTGTCCCTTTTG	TTGGCTGAGTGGTAGAGTCCC
MMP8	TCTTCCTCCACACACAGCTTG	CTGCAACCATCGTGGCATTC
MMP9	CTGGACAGCCAGACACTAAAG	CTCGCGGCAAGTCTTCAGAG
CCL2	TTAAAAACCTGGATCGGAACCAA	GCATTAGCTTCAGATTTACGGGT
CCL8	TCTACGCAGTGCTTCTTTGCC	AAGGGGGATCTTCAGCTTTAGTA
CXCL15	TCGAGACCATTTACTGCAACAG	CATTGCCGGTGGAAATTCCTT
VCAM1	AGTTGGGGATTCGGTTGTTCT	CCCCTCATTCCTTACCACCC
GAPDH	AGGTCGGTGTGAACGGATTTG	TGTAGACCATGTAGTTGAGGTCA

blocked with 5% (w/v) skimmed milk and then incubated at 4 °C overnight with the following primary antibodies: Phospho-Akt (1:1000, #13,038 Cell Signaling Technology, USA), Akt (1:1000, #4691 Cell Signaling Technology), and GAPDH (1:1000, TA08 ZSGB-BIO, China). The following day, the membranes were incubated with infrared Dye 800-conjugated secondary antibodies (Rockland Immunochemicals, Inc., Pa.) for 1 h at room temperature. The blot images were subsequently obtained and quantified using an Odyssey infrared imaging system (LI-COR Biosciences, NE).

Mice and Vascular Wall Softening Model

All animal studies were approved by the Animal Research Ethics Committee of Capital Medical University and conformed to the National Institutes of Health's Guide for the Care and Use of Laboratory Animals. Vascular wall softening model was generated in 3-week-old male C57BL/6 mice via administration of BAPN at 1 g/kg/day (Sigma-Aldrich) in the drinking water for 4 weeks.

Atomic Force Microscopy (AFM)

Mouse aortas were embedded in optimal cutting temperature (OCT) compound, frozen, and cut into 20-μm-thick sections for AFM analysis. The aortas were probed using a DNP-10D tip (Bruker, USA, nominal stiffness ~ 0.06 N/m) on a Bruker Dimension Icon AFM. Probe deflection sensitivity was calibrated by taking indentation curves on glass and the nominal tip stiffness was calibrated by thermal tuning. Force versus deflection curves were generated for a ramp size of 1 μm from at least five locations per tissue sample. The first 400 nm of the extension curves were fitted using NanoScope Analysis Software version 1.4 (Bruker) assuming a Poisson ratio of 0.5 and using the Sneddon fit model [19].

Mechanical Tensile Testing

The procedures used for uniaxial tensile testing and analyses have been reported previously [20]. We measured the tensile properties of aortic rings using a mechanical tensile tester. Prior to stretching, the aortic ring was placed over two stainless hooks with a diameter of 0.25 mm. Both ends of the stainless hooks were clamped, and the clamps were connected to the force sensor with an accuracy of 0.0002 N. The rings were stretched uniaxially in saline at 37 °C using sensors and a thermostatically controlled heating plate at a rate of 0.05 mm/s. Throughout the stretching process, photographs were taken to monitor the changes in ring conformation. After stretching, the distance between the two hooks was determined in each photograph, and from this measurement the local stretch ratio was calculated. The post-processing of data was based on a previously described method, which takes into consideration the double vessel wall structure of rings when placed over two hooks.

Aortic Diameter Measurements

At 28 days after BAPN administration, two-dimensional B-mode ultrasound (US) imaging was performed to determine the diameter of the thoracic aorta of mice. US image analysis was performed using the accompanying Vevo2100 software (VisualSonics, Canada). For each mouse, three measurements were taken, with the investigator being blinded to the experimental groups.

Elastic Fiber Staining

Mouse aortas were harvested at designated time points, embedded in OCT, and 5-μm cryosections were cut for elastin staining following the manufacturer's instructions (MXB, China). Aortic sections were examined by four

independent observers who were blinded to the animal group allocation. All images were recorded using a Nikon Eclipse TE2000-S microscope (Nikon, Japan).

Statistical Analysis

Data are expressed as the mean ± SEM. All experiments were repeated at least three times with representative data shown. Comparisons of means between two groups were performed using unpaired two-tailed Student *t*-tests. More than two groups were compared by two-way analysis of variance (ANOVA) with Bonferroni post hoc analysis. Kaplan–Meier survival curves were used to analyze the survival percentages. P values < 0.05 were considered to indicate statistical significance. Analyses were performed using Prism 7 software (GraphPad Software Inc., USA).

Results

ECM Softening Promotes VSMC Dedifferentiation Toward a Synthetic Phenotype

To explore the effects of ECM stiffness on phenotypic modulation in VSMCs, VSMCs were cultured in Matrix hydrogels with different stiffnesses containing a mix of Matrigel and 1.2 or 3 mg/mL collagen I (elastic modulus: 0.17 or 1.2 kPa, respectively) [16–18] (Fig. 1a). Transcriptome sequencing was performed to comprehensively evaluate gene expression in VSMCs in response to the soft and stiff Matrix hydrogel. Finally, 474 differentially expressed genes (DEGs), among which 304 were upregulated and 173 were down-regulated (filtering criteria adjusted P value < 0.05, the absolute value of fold change > 1.2) were obtained in VSMCs cultured in soft ECM. To gain insight into the phenotypic alteration of VSMCs, we performed gene ontology (GO) enrichment analysis using DAVID. Interestingly, the top 2 groups of

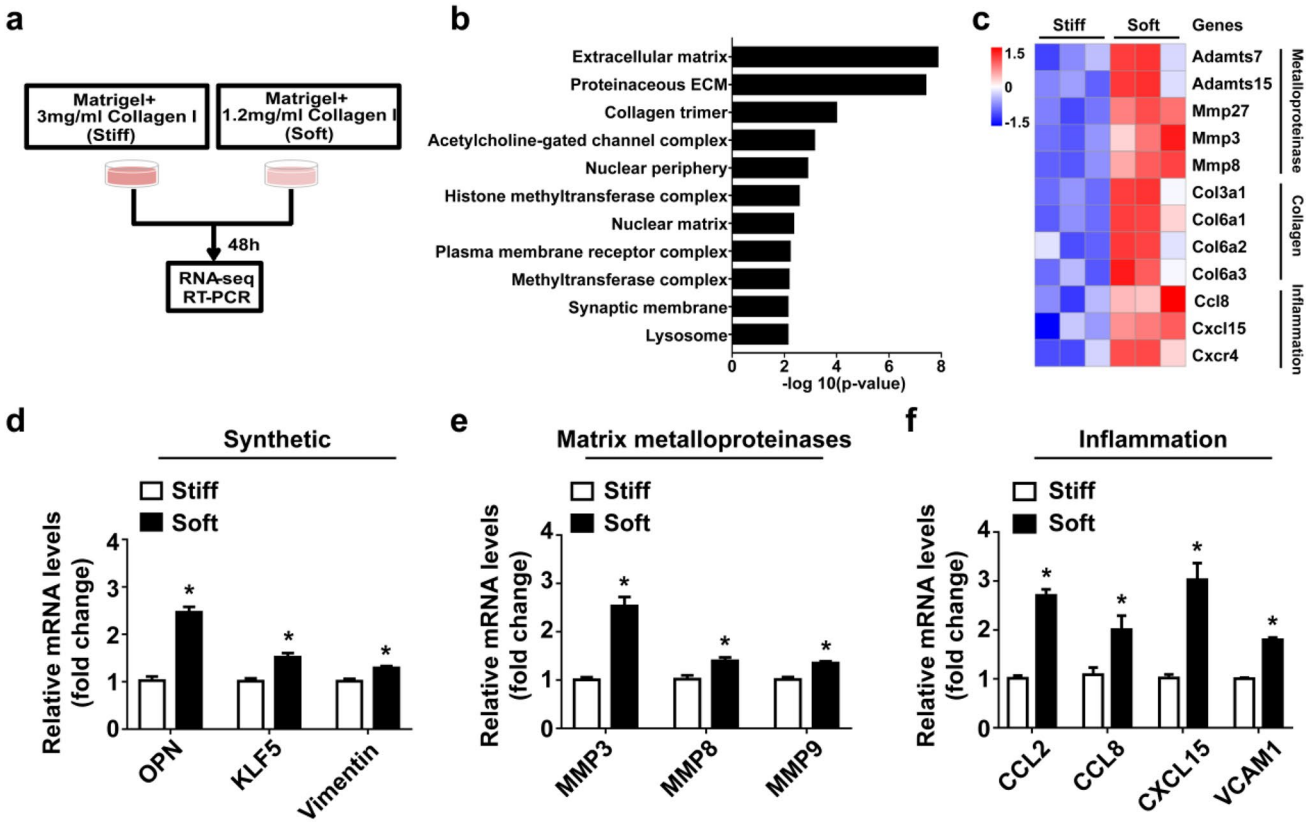

Fig. 1 ECM softening leads to a synthetic VSMC phenotype in vitro. **a** VSMCs were embedded in a matrix comprising different mixtures of Matrigel and collagen I. Stiff and soft matrix hydrogels contained 3 and 1.2 mg/mL Collagen I, respectively. After 48 h, the cells were harvested for RNA-seq or RT-PCR. **b** Gene ontology (GO) analysis (cellular component) of upregulated genes in VSMCs cultured in soft ECM vs. stiff ECM. **c** Heatmap of the mean normalized expression of the selected genes in VSMCs cultured in stiff and soft Matrix hydrogel by RNA-seq (**d**–**f**) RT-PCR analysis of the expression of synthetic, MMPs, and inflammatory marker genes in VSMCs grown in stiff and soft Matrix hydrogel ($n = 6$). *$P < 0.05$ relative to Stiff samples. Data are expressed as the mean ± SEM

upregulated genes were involved in extracellular matrix (GO: 0031012) and proteinaceous extracellular matrix (GO: 0005578) (Fig. 1b); particularly, the most upregulated genes were clusters of metalloproteinase genes and collagen genes (Fig. 1c), which is a characteristic profile for synthetic VSMCs [3, 21, 22]. Furthermore, quantitative PCR verified the upregulation of synthetic phenotype-related genes (osteopontin, KLF5, vimentin, matrix metalloproteinases (MMPs), and inflammatory cytokines) in VSMCs following ECM softening (Fig. 1d–f). Collectively, these results indicate that ECM softening induces a synthetic phenotype in VSMCs.

ECM Softening Actives AKT Phosphorylation

To investigate the potential mechanism by which ECM softening regulates VSMC synthetic phenotype switching, we performed pathway analysis of the DEGs obtained through transcriptome sequencing as described above which revealed activation of the Toll-like signaling pathway and PI3K/AKT signaling pathway in VSMCs cultured in soft Matrix hydrogel (Fig. 2a). Next, we confirmed activation of the PI3K/AKT pathway by western blot analysis of AKT phosphorylation. The level of phosphorylated AKT was significantly increased in VSMCs cultured in soft ECM as compared with that in stiff ECM (Fig. 2b, c). Given that PI3K/AKT has been suggested as an important signaling pathway that induces VSMCs phenotype switching, PI3K/AKT signaling activation may be responsible for ECM softening-induced VSMC synthetic phenotype switching.

LOX Inhibitor Promotes Vascular Wall ECM Softening In Vivo

To gain insight into the in vivo relationship between ECM stiffness and VSMC function, we developed an animal model with decreased ECM stiffness. As described previously, collagen is the most abundant scaffolding protein in the ECM, and increasing content and cross-linking of collagen enhance ECM stiffness. In contrast, aberrant collagen cross-linking may contribute to decreased ECM stiffness. Lysyl oxidase (LOX) is responsible for collagen cross-linking, and loss-of-function mutation in LOX has been demonstrated to disturb the cross-linking of collagen and elastin and lead to the formation of aortic aneurysm/dissection in humans [23]. Therefore, we administered the LOX inhibitor BAPN to mice to construct an ECM softening model in vivo. Vascular stiffness was evaluated at 7, 14, 21, and 28 days after BAPN administration. The aortic rings isolated from BAPN- administered mice were first evaluated by an ex vivo aortic ring tensile test to measure vascular stiffness [24]. The circumferential stress in the range of the tensile length was determined, and then stress–strain curves were generated to evaluate the tangential elastic stiffness. The stress–strain

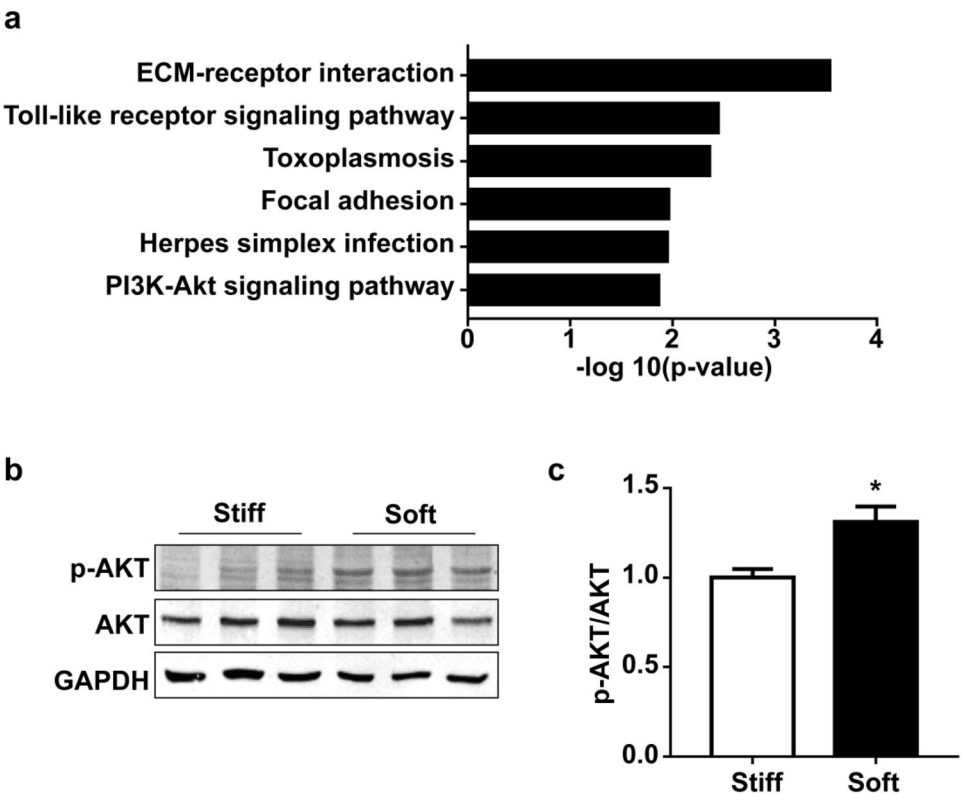

Fig. 2 ECM softening induces AKT phosphorylation. **a** Enriched KEGG signaling pathways for upregulated genes in VSMCs cultured in soft Matrix hydrogel relative to in stiff Matrix hydrogel identified by RNA-seq. **b**, **c** Representative western blot and quantification of p-AKT and AKT in VSMCs grown in stiff and soft Matrix hydrogels ($n=3$) $^{*}P<0.05$ versus stiff. Data are expressed as the mean ± SEM

curves clearly revealed that the stiffness of the thoracic aortas was significantly decreased in response to BAPN administration (Fig. 3a, b). AFM nanoindentation was performed to examine the medial layer of the thoracic aorta after BAPN administration. We observed that the deflection signal of the cantilever increased to a slightly greater extent in the BAPN group than in the control group (i.e., a slower bending of the cantilever indicates less stiffness; 15.72 ± 6.66 vs. 36.98 ± 18.11 kPa, respectively) (Fig. 3c, d) [6, 25]. Furthermore, elastic fiber staining revealed a disturbed aortic structure and degradation of aortic elastic fibers after BAPN administration (Fig. 3e). Together, these data demonstrate the successful induction of vascular wall softening after BAPN administration.

ECM Softening Regulates VSMC Phenotypic Switching In Vivo

To comprehensively define gene expression in the aortas following BAPN administration, we performed transcriptome sequencing of the aortas from control and BAPN-treated mice. Consistent with the in vitro results, the levels of synthetic phenotype-related genes (MMPs, collagens and inflammatory cytokines) were upregulated (Fig. 4a). Accordingly, quantitative PCR verified upregulation of the synthetic phenotype-related genes OPN, vimentin, and MMP3 in the softened aortas of mice (Fig. 4b). These data indicate that the VSMCs tended toward synthetic phenotypes in the in vivo ECM softening model. Finally, we observed that the

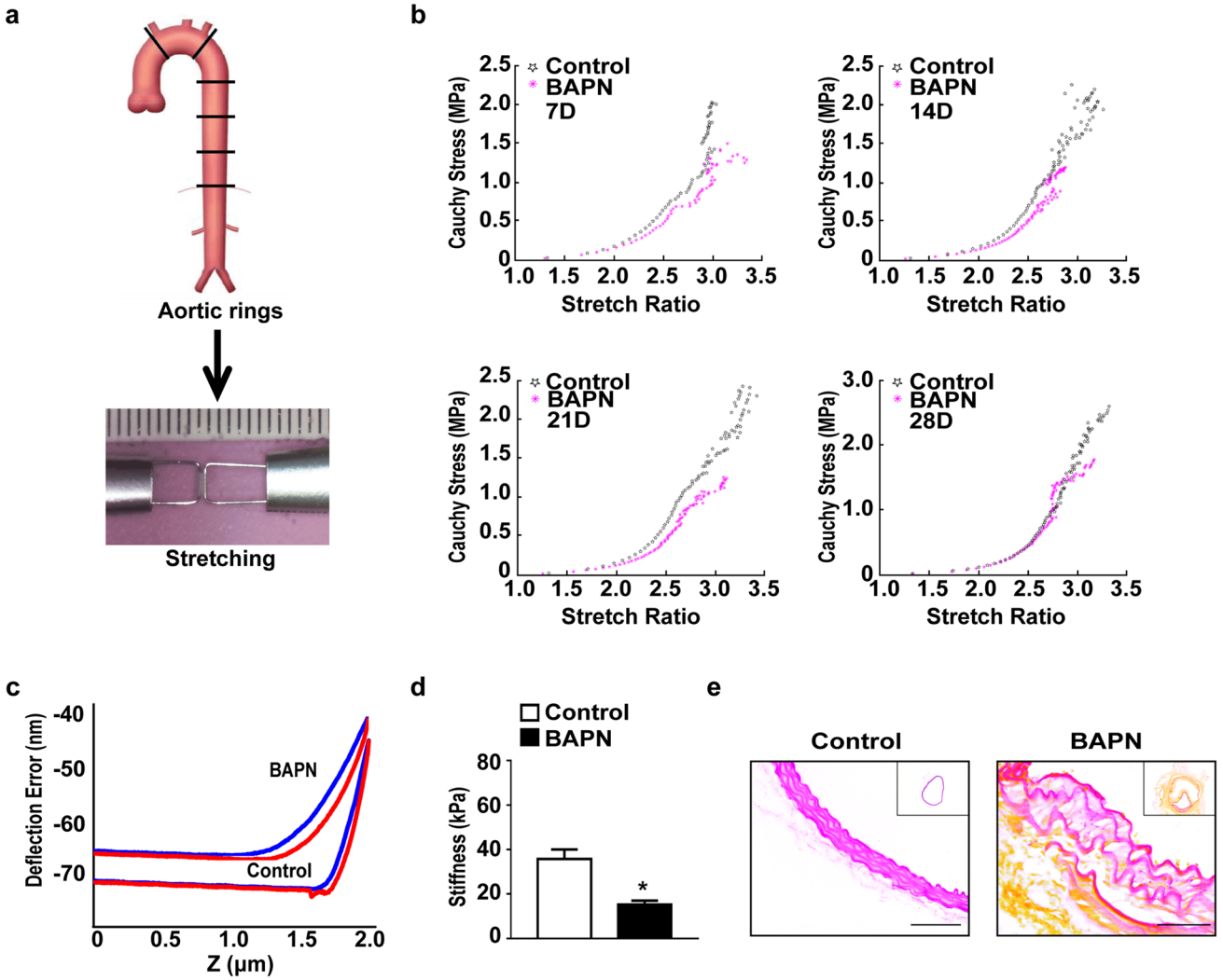

Fig. 3 Inhibition of LOX activity promotes vascular wall softening. **a** Schematic of experimental workflow for mechanical tensile testing. **b** Excised aortic rings from control and BAPN-administered mice were mechanically stretched, and stiffness was determined from the stress–strain relationship, as shown for representative rings ($n = 6$). **c** and **d** The stiffness of thoracic aortas was determined by atomic force microscopy (AFM) nanoindentation. The deflection signal from the AFM cantilever was recorded, as shown for the representative approach (blue) and retraction (red) curves. $^*P < 0.05$ versus control. **e** Representative aortic elastic fiber staining in control or BAPN-administered mice ($n = 6$). Scale bars, 50 μm. Data are expressed as the mean ± SEM

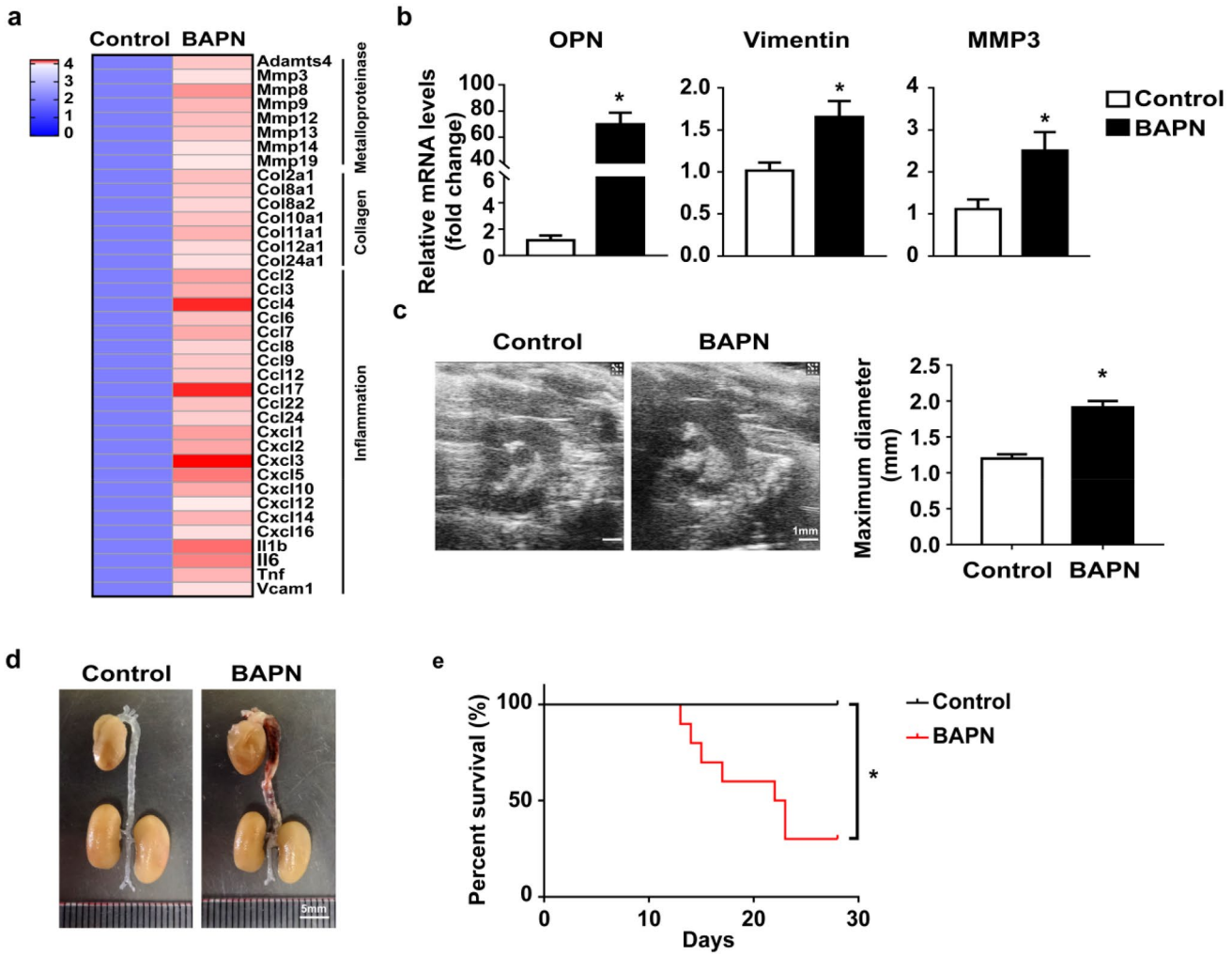

Fig. 4 VSMC switched to synthetic phenotype in softened aortas of mice. **a** Heatmap showing the mean normalized expression of transcripts encoding the synthetic and pro-inflammatory phenotype-related genes. RNA-sequencing data are from the control and BAPN-administered mouse aortas. **b** RT-PCR analysis in control and BAPN-administered mice to determine the expression of synthetic phenotype-related genes ($n=6$). $^*P<0.05$ versus control. Data are expressed as the mean ± SEM; unpaired two-tailed Student *t*-tests. **c** Ultrasound images of the luminal diameter of the ascending aorta in mice with or without BAPN administration ($n=6$). Scale bars, 1 mm. $^*P<0.05$ versus control. Data are expressed as the mean ± SEM; unpaired two-tailed Student *t*-tests. **d** Representative images of whole aortas in mice with or without BAPN administration ($n=6$) Scale bars, 5 mm. **e** Kaplan–Meier survival curves of control and BAPN-administered mice ($n=10$). $^*P<0.05$ versus control

aortas in BAPN-treated mice underwent severe expansion and developed thoracic aortic dissection (TAD) (Fig. 4c–e).

Discussion

In this study, we demonstrated that vascular wall softening as a result of aberrant collagen cross-linking or ECM degradation under pathological conditions promoted synthetic phenotype switching in VSMCs and triggered the occurrence of aortic dissection.

Cells sense physical forces, such as changes in ECM stiffness, and translate these stimuli into biochemical signals, which contributing to physiological and pathological processes in multiple organs [26]. Herein, unbiased transcriptomic analyses of in vitro and in vivo models revealed that ECM softening-induced synthetic phenotype switching in VSMCs. As the stiffness of the vascular wall gradually decreased over time, VSMCs tended to develop synthetic and pro-inflammatory phenotypes. Previous studies showed that changes in vascular wall stiffness promoted calcific phenotypic transition of VSMCs [25]. In contrast to the softer matrix hydrogel (0.17–1.2 kPa) used in the present study, artificial polyacrylamide gels with considerably higher stiffness (2.16–16.75 kPa) have been used previously to culture VSMCs. The extremely

rigid matrix hydrogel used in earlier studies mimicked vascular calcification, which promoted the differentiation of VSMCs into osteoblasts. Therefore, under different pathological conditions, excessive softening or stiffening of the ECM perturbs VSMC homeostasis.

Regulation of VSMC phenotype is a multifactorial process involving the myocardin-serum response factor (SRF) complex and several signaling pathways. SRF and the coactivator gene myocardin interact with the CArG elements within the promoter region of VSMC marker gene to drive its expression [27]. This interaction can be competed with phosphorylated Elk-1, which is activated by ERK1/2 or PI3K/AKT pathways, resulting in inhibition of SRF-myocardin for CArG binding and dedifferentiation of VSMC [28, 29]. Thus, activation of PI3K/AKT may contribute to VSMC dedifferentiation in an Elk-1 dependent manner. Addition, PI3K/AKT signaling pathway has been known to play important roles in cell proliferation, migration, and other cell processes [6, 30, 31]. AKT activation down-regulates VSMC markers in dedifferentiated mesenchymal progenitor cells, whereas inhibition of PI3K could reverse the dedifferentiated phenotype by inducing the expression of calponin, α-smooth muscle actin, and SM22α [32, 33]. Considering its critical function in VSMC dedifferentiation, activation of PI3K/AKT signaling may be responsible for ECM softening-induced VSMC synthetic phenotype switching.

We also demonstrated that administration of the LOX inhibitor BAPN induced vascular wall softening, leading to aortic dissection. Although previous studies revealed an increase in the arterial stiffness in patients with Marfan syndrome (characterized by aortic aneurysm/dissection) [34], this is likely a late remodeling process that occurs after destruction and dilation of the aorta. In BAPN-treated mice, we observed dynamic changes during different disease stages, characterized by softening in the early stages but stiffening in the later stages. Mutations in LOX and collagen (COL14A1/COL6A5/COL5A2) genes have also been detected in patients with aortic dissection [23, 35, 36], which may be explained by de-cross-linking of collagens, degradation of the ECM, and vascular wall softening, subsequently accelerating the occurrence of aortic dissection. This suggests that early vascular wall softening initiates aortic injury to promote synthetic phenotype switching of VSMCs and the development of aortic dissection, eventually leading to abnormal remodeling.

In summary, we demonstrated that ECM degradation can soften vascular walls, promoting VSMC shift to the synthetic phenotype during TAD. The present work indicates that ECM softening is an early TAD trigger, providing valuable insights into the associations among ECM softening, VSMC function, and vascular homeostasis.

Acknowledgements This work was supported by grants from the National Natural Science Foundation of China (81930014 to J.D., and 81870339 to P.L.).

Author Contributions JD, PL, HRL and YLL: conceived and supervised the study. YHS and SH performed and analyzed in vivo experiments. YHS, GQL, and BKQ: performed the in vitro experiments and analyzed the data. ZFL, DDC: provided technical assistance. JD, PL, HRL, and YHS: wrote the manuscript with inputs from co-authors.

Compliance with Ethical Standards

Conflict of interest There are no conflict to declare.

References

1. Rodriguez, A. I., Csanyi, G., Ranayhossaini, D. J., Feck, D. M., Blose, K. J., Assatourian, L., et al. (2015). MEF2B-Nox1 signaling is critical for stretch-induced phenotypic modulation of vascular smooth muscle cells. *Arteriosclerosis, Thrombosis, and Vascular Biology, 35*(2), 430–438. https://doi.org/10.1161/ATVBAHA.114.304936.
2. Zhang, M. J., Zhou, Y., Chen, L., Wang, Y. Q., Wang, X., Pi, Y., et al. (2016). An overview of potential molecular mechanisms involved in VSMC phenotypic modulation. *Histochemistry and Cell Biology, 145*(2), 119–130. https://doi.org/10.1007/s00418-015-1386-3.
3. Liu, R., Lo, L., Lay, A. J., Zhao, Y., Ting, K. K., Robertson, E. N., et al. (2017). ARHGAP18 protects against thoracic aortic aneurysm formation by mitigating the synthetic and proinflammatory smooth muscle cell phenotype. *Circulation Research, 121*(5), 512–524. https://doi.org/10.1161/CIRCRESAHA.117.310692.
4. Yang, L., Gao, L., Nickel, T., Yang, J., Zhou, J., Gilbertsen, A., et al. (2017). Lactate promotes synthetic phenotype in vascular smooth muscle cells. *Circulation Research, 121*(11), 1251–1262. https://doi.org/10.1161/CIRCRESAHA.117.311819.
5. Desai, A., Geraghty, S., & Dean, D. (2019). Effects of blocking integrin beta1 and N-cadherin cellular interactions on mechanical properties of vascular smooth muscle cells. *Journal of Biomechanics, 82*, 337–345. https://doi.org/10.1016/j.jbiomech.2018.11.004.
6. Wang, H., Tibbitt, M. W., Langer, S. J., Leinwand, L. A., & Anseth, K. S. (2013). Hydrogels preserve native phenotypes of valvular fibroblasts through an elasticity-regulated PI3K/AKT pathway. *Proceedings of the National Academy of Sciences of the United States of America, 110*(48), 19336–19341. https://doi.org/10.1073/pnas.1306369110.
7. Halper, J., & Kjaer, M. (2014). Basic components of connective tissues and extracellular matrix: Elastin, fibrillin, fibulins, fibrinogen, fibronectin, laminin, tenascins and thrombospondins. *Advances in Experimental Medicine and Biology, 802*, 31–47. https://doi.org/10.1007/978-94-007-7893-1_3.
8. Didangelos, A., Yin, X., Mandal, K., Baumert, M., Jahangiri, M., & Mayr, M. (2010). Proteomics characterization of extracellular space components in the human aorta. *Molecular & Cellular Proteomics : MCP, 9*(9), 2048–2062. https://doi.org/10.1074/mcp.M110.001693.
9. Kandalam, V., Basu, R., Moore, L., Fan, D., Wang, X., Jaworski, D. M., et al. (2011). Lack of tissue inhibitor of metalloproteinases 2 leads to exacerbated left ventricular dysfunction and adverse extracellular matrix remodeling in response to biomechanical stress. *Circulation, 124*(19), 2094–2105. https://doi.org/10.1161/circulationaha.111.030338.

10. Chen, J. H., & Simmons, C. A. (2011). Cell-matrix interactions in the pathobiology of calcific aortic valve disease: Critical roles for matricellular, matricrine, and matrix mechanics cues. *Circulation Research, 108*(12), 1510–1524. https://doi.org/10.1161/CIRCRESAHA.110.234237.
11. Najafi, M., Farhood, B., & Mortezaee, K. (2019). Extracellular matrix (ECM) stiffness and degradation as cancer drivers. *Journal of Cellular Biochemistry, 120*(3), 2782–2790. https://doi.org/10.1002/jcb.27681.
12. Moro, A., Driscoll, T. P., Boraas, L. C., Armero, W., Kasper, D. M., Baeyens, N., et al. (2019). MicroRNA-dependent regulation of biomechanical genes establishes tissue stiffness homeostasis. *Nature Cell Biology, 21*(3), 348–358. https://doi.org/10.1038/s41556-019-0272-y.
13. Gu, Z., Liu, F., Tonkova, E. A., Lee, S. Y., Tschumperlin, D. J., & Brenner, M. B. (2014). Soft matrix is a natural stimulator for cellular invasiveness. *Molecular Biology of the Cell, 25*(4), 457–469. https://doi.org/10.1091/mbc.E13-05-0260.
14. Liu, F., Mih, J. D., Shea, B. S., Kho, A. T., Sharif, A. S., Tager, A. M., et al. (2010). Feedback amplification of fibrosis through matrix stiffening and COX-2 suppression. *The Journal of Cell Biology, 190*(4), 693–706. https://doi.org/10.1083/jcb.201004082.
15. Chen, Y., Budd, R. C., Kelm, R. J., Jr., Sobel, B. E., & Schneider, D. J. (2006). Augmentation of proliferation of vascular smooth muscle cells by plasminogen activator inhibitor type 1. *Arteriosclerosis, Thrombosis, and Vascular Biology, 26*(8), 1777–1783. https://doi.org/10.1161/01.ATV.0000227514.50065.2a.
16. Paszek, M. J., Zahir, N., Johnson, K. R., Lakins, J. N., Rozenberg, G. I., Gefen, A., et al. (2005). Tensional homeostasis and the malignant phenotype. *Cancer Cell, 8*(3), 241–254. https://doi.org/10.1016/j.ccr.2005.08.010.
17. Aragona, M., Panciera, T., Manfrin, A., Giulitti, S., Michielin, F., Elvassore, N., et al. (2013). A mechanical checkpoint controls multicellular growth through YAP/TAZ regulation by actin-processing factors. *Cell, 154*(5), 1047–1059. https://doi.org/10.1016/j.cell.2013.07.042.
18. Bertero, T., Cottrill, K. A., Lu, Y., Haeger, C. M., Dieffenbach, P., Annis, S., et al. (2015). Matrix remodeling promotes pulmonary hypertension through feedback mechanoactivation of the YAP/TAZ-miR-130/301 circuit. *Cell Reports, 13*(5), 1016–1032. https://doi.org/10.1016/j.celrep.2015.09.049.
19. Sunyer, R., Conte, V., Escribano, J., Elosegui-Artola, A., Labernadie, A., Valon, L., et al. (2016). Collective cell durotaxis emerges from long-range intercellular force transmission. *Science, 353*(6304), 1157–1161. https://doi.org/10.1126/science.aaf7119.
20. Teng, Z., Zhang, Y., Huang, Y., Feng, J., Yuan, J., Lu, Q., et al. (2014). Material properties of components in human carotid atherosclerotic plaques: A uniaxial extension study. *Acta Biomaterialia, 10*(12), 5055–5063. https://doi.org/10.1016/j.actbio.2014.09.001.
21. Branchetti, E., Poggio, P., Sainger, R., Shang, E., Grau, J. B., Jackson, B. M., et al. (2013). Oxidative stress modulates vascular smooth muscle cell phenotype via CTGF in thoracic aortic aneurysm. *Cardiovascular Research, 100*(2), 316–324. https://doi.org/10.1093/cvr/cvt205.
22. Ding, Y., Zhang, M., Zhang, W., Lu, Q., Cai, Z., Song, P., et al. (2016). AMP-activated protein kinase alpha 2 deletion induces VSMC phenotypic switching and reduces features of atherosclerotic plaque stability. *Circulation Research, 119*(6), 718–730. https://doi.org/10.1161/CIRCRESAHA.116.308689.
23. Lee, V. S., Halabi, C. M., Hoffman, E. P., Carmichael, N., Leshchiner, I., Lian, C. G., et al. (2016). Loss of function mutation in LOX causes thoracic aortic aneurysm and dissection in humans. *Proceedings of the National Academy of Sciences of the United States of America, 113*(31), 8759–8764. https://doi.org/10.1073/pnas.1601442113.
24. Sehgel, N. L., Sun, Z., Hong, Z., Hunter, W. C., Hill, M. A., Vatner, D. E., et al. (2015). Augmented vascular smooth muscle cell stiffness and adhesion when hypertension is superimposed on aging. *Hypertension, 65*(2), 370–377. https://doi.org/10.1161/HYPERTENSIONAHA.114.04456.
25. Xie, S. A., Zhang, T., Wang, J., Zhao, F., Zhang, Y. P., Yao, W. J., et al. (2018). Matrix stiffness determines the phenotype of vascular smooth muscle cell in vitro and in vivo: Role of DNA methyltransferase 1. *Biomaterials, 155*, 203–216. https://doi.org/10.1016/j.biomaterials.2017.11.033.
26. Mierke, C. T. (2011). The biomechanical properties of 3d extracellular matrices and embedded cells regulate the invasiveness of cancer cells. *Cell Biochemistry and Biophysics, 61*(2), 217–236. https://doi.org/10.1007/s12013-011-9193-5.
27. Owens, G. K., Kumar, M. S., & Wamhoff, B. R. (2004). Molecular regulation of vascular smooth muscle cell differentiation in development and disease. *Physiological Reviews, 84*(3), 767–801. https://doi.org/10.1152/physrev.00041.2003.
28. Lin, C.-C., Lin, W.-N., Cheng, S.-E., Tung, W.-H., Wang, H.-H., & Yang, C.-M. (2012). Transactivation of EGFR/PI3K/Akt involved in ATP-induced inflammatory protein expression and cell motility. *Journal of Cellular Physiology, 227*(4), 1628–1638. https://doi.org/10.1002/jcp.22880.
29. Zhang, Q., Adiseshaiah, P., Kalvakolanu, D. V., & Reddy, S. P. (2006). A Phosphatidylinositol 3-kinase-regulated Akt-independent signaling promotes cigarette smoke-induced FRA-1 expression. *The Journal of Biological Chemistry, 281*(15), 10174–10181. https://doi.org/10.1074/jbc.M513008200.
30. Vega, R. B., Konhilas, J. P., Kelly, D. P., & Leinwand, L. A. (2017). Molecular mechanisms underlying cardiac adaptation to exercise. *Cell Metabolism, 25*(5), 1012–1026. https://doi.org/10.1016/j.cmet.2017.04.025.
31. Zhang, M., Li, F., Wang, X., Gong, J., Xian, Y., Wang, G., et al. (2020). MiR-145 alleviates Hcy-induced VSMC proliferation, migration, and phenotypic switch through repression of the PI3K/Akt/mTOR pathway. *Histochemistry and Cell Biology*. https://doi.org/10.1007/s00418-020-01847-z.
32. Hegner, B., Lange, M., Kusch, A., Essin, K., Sezer, O., Schulze-Lohoff, E., et al. (2009). mTOR regulates vascular smooth muscle cell differentiation from human bone marrow-derived mesenchymal progenitors. *Arteriosclerosis, Thrombosis, and Vascular Biology, 29*(2), 232–238. https://doi.org/10.1161/ATVBAHA.108.179457.
33. Zhang, L., Xie, P., Wang, J., Yang, Q., Fang, C., Zhou, S., et al. (2010). Impaired peroxisome proliferator-activated receptor-gamma contributes to phenotypic modulation of vascular smooth muscle cells during hypertension. *The Journal of Biological Chemistry, 285*(18), 13666–13677. https://doi.org/10.1074/jbc.M109.087718.
34. Perrucci, G. L., Rurali, E., Gowran, A., Pini, A., Antona, C., Chiesa, R., et al. (2017). Vascular smooth muscle cells in Marfan syndrome aneurysm: The broken bricks in the aortic wall. *Cellular and Molecular Life Sciences : CMLS, 74*(2), 267–277. https://doi.org/10.1007/s00018-016-2324-9.
35. Li, Z., Zhou, C., Tan, L., Chen, P., Cao, Y., Li, C., et al. (2017). Variants of genes encoding collagens and matrix metalloproteinase system increased the risk of aortic dissection. *Science China Life Sciences, 60*(1), 57–65. https://doi.org/10.1007/s11427-016-0333-3.
36. Guo, D. C., Regalado, E. S., Gong, L., Duan, X., Santos-Cortez, R. L., Arnaud, P., et al. (2016). LOX mutations predispose to thoracic aortic aneurysms and dissections. *Circulation Research, 118*(6), 928–934. https://doi.org/10.1161/CIRCRESAHA.115.307130.